FERMILAB-Proposal-0480

Proposal to Search for Heavy Bosons, Heavy Leptons, and Charmed Particles at SSR

Luke W. Mo*, Peter E. Schlein, and Andris Skuja

The University of Chicago*, UCLA, and the University of Oxford

*Spokesman, present address.

26 pp.

I. Introduction

Recently a proposal to build a small storage ring (SSR) of 25 GeV in collision with the main ring has been presented at Fermilab (FNAL Proposal 478 by R. Huson, P. Livdahl, R. Steining, L. Teng, and J.K. Walker). The proposed machine will have an intersection region 18.84 m in length, with a corresponding luminosity of 10^{31} to 10^{32} cm^{-2} sec^{-1}, with center of mass energies ranging from 25 GeV to 200 GeV. The experimenters of P-478 propose to search for intermediate boson production by observing single muons at large transverse momenta. Muon pairs in which both muons will have transverse momenta in excess of 1 GeV will also be observed. The detector consists of a cylinder 1.2 meters in radius, stacked from drift chambers and toroidally magnetized iron sandwiches. It will cover the entire 18.84 m length of the interaction region.

We are excited by this novel idea of building a small storage ring and wish to express our strongest support for it. We feel that the SSR will lead to a new understanding of fundamental physics as well as maintain the impetus of opening up new frontiers in elementary particle physics at Fermilab.

The experiment we propose to do on the SSR is to search for heavy bosons, heavy leptons, and charmed particles. The hadrons associated with the production of these heavy particles will also be detected. We emphasize the importance of measuring the hadronic system which should help to determine the properties of the new particles. The signature for the processes in which we are interested are characterized by charged lepton pairs in the final state. The three processes we want to investigate are:

$$(1) \qquad p + p \rightarrow (\gamma^* \text{ or } Z^0) + X \longrightarrow \begin{cases} e^+ + e^- \\ \mu^+ + \mu^- \end{cases}$$

$$(2) \qquad p + p \rightarrow (L^+ + L^-) + X, \quad L^- \longrightarrow \ell^- + \bar{\nu}_\ell + \nu_L, \quad L^+ \longrightarrow \ell^+ + \nu_\ell + \bar{\nu}_L$$

$$(3) \qquad p + p \rightarrow D + \bar{D} + X, \quad \bar{D} \longrightarrow \mu + \nu_\mu + \dots, \quad D \longrightarrow e + \nu_e + \dots$$

By measuring the electron pairs or muon pairs in the final state, one can discover particles of heavy mass. By measuring the combination of (μ^+e^-) or (μ^-e^+) one can discover the long-sought after heavy leptons and charmed particles. Measurement of hadrons associated with the heavy particle production should help to determine the properties of these new particles.

We stress the importance of the SSR in this particle search, since the production cross-sections for high mass particles increase rapidly with an increase of the center of mass energy.

II. Experimental Apparatus

A. The Spectrometer

The spectrometer we propose for this heavy particle search consists of a wheel-shaped super-conducting magnet, sets of drift chambers, scintillation counter hodoscopes, and a lead glass hodoscope. The main consideration that enters into the spectrometer design are the following:

(1) The field of the spectrometer magnet should be transverse to the beam direction. This maximizes the analyzing power of the magnet.

(2) The spectrometer should be able to detect electrons as well as muons, since it is the combination of (μ^+e^-) or (μ^-e^+) that provide the best signature for pair production of heavy leptons and charmed particles. We note that electrons, unlike muons, do not originate from charged pion decay, even though they can arise from Kaon decay or the Dalitz decay of neutral pions. This lack of electron decay products reduces the contamination to the (e^+e^-) and (μe) samples. On the other hand, the ($\mu^+\mu^-$) sample would still suffer from muons originating from pion decay.

(3) The spectrometer should be capable of detecting the hadrons associated with the production of the heavy particle.

(4) The production angle and momenta of the particles should be measured with good accuracy. Also, the spectrometer should have good acceptance for the detection of electrons and muons.

A spectrometer possessing these characteristics is shown in Figure 1a. *The spectrometer covers one third of the interaction region. A set of 16* drift-chambers planes (2m x 2m) are placed before the magnet to measure the particle production angles. Another set of 16 drift chamber planes of the same size are placed behind the magnet to measure the exit path of the particle leaving the magnet. Around the magnet, each one of the six air gaps will be covered by 8 drift chamber planes of size 2m x 70 cm to measure the charged hadron tracks. Two scintillation counter hodoscopes are placed immediately at the entrance and exit faces of the magnet (between the magnet and the two sets of drift chambers). Scintillation counters will be placed at appropriate positions upstream and downstream of the interaction region to insure the occurrence of beam - beam interactions by detecting particles going along opposite directions. Finally, the lead glass hodoscope is placed at the end of the spectrometer.

The electrons and positrons are detected by the lead glass hodoscope. The muons are detected by the scintillation counter hodoscope immediately behind the iron of the magnet. The hodoscope placed in front of the magnet is used to improve the background and time resolution of the spectrometer. Additional details of each of the components of the spectrometer are discussed below:

(1) <u>The Magnet</u>

The magnet is constructed from six steel wedges and six air gaps, arranged into the shape of a wheel. It is energized by superconducting coils. It has a diameter of 2m and a length of 2m. Since the magnet sits at one end of the interaction region and the particles to be detected pass through axially, the beam pipe can easily be shielded adequately.

An end view of the magnet is shown in Figure 1b. The magnet design is underway. We will submit an addendum on it and the cost estimate at a later time.

(2) <u>The Drift Chambers</u>

We propose to build 32 drift chambers of dimension 2m x 2m. Each chamber is split into two sections as shown in Figure 2a. A hole in the middle of the chamber will accommodate the beam pipe. In addition, because of this hole, particles such as pions produced at high rates in p-p collisions, at small $p_\perp$, will remain undetected. The chambers will be split into two sections, to allow for quick installation and repair (the latter is especially important during the data taking phase when pressure to run is high).

The mechanical construction of the drift chamber is shown schematically in Figure 2b. They are economic and easy to build. The sense wires of the drift chamber will be spaced 2 cm apart. We plan to install two sets of horizontal and two sets of vertical wires in one box. We estimate that the cost per wire plane will be approximately \$4000 (\$500 for mechanical construction and \$3500 for electronics and readout).

It should be noted that we plan to measure straight lines before and after the momentum analyzing magnet. We have already learned how to deal with the problem of pattern recognition from our experience gained on multiparticle experiments conducted at Fermilab and CERN-ISR. We do not consider it difficult to adapt our knowledge to the present experiment.

We will also insert a few sets of drift chambers or MWPC's inside the air gaps of the magnet to provide additional redundancy. The charged particles emerging from the side of the magnet will be measured by drift chambers outside the air gaps. Each one of the six air gaps will be covered by eight drift wire planes of size 2m x 70 cm.

(3) The Scintillation Counter Hodoscopes

The scintillation counter hodoscopes, located immediately before and after the magnet, will consist of 48 counters each arranged in a wheel shaped pattern to match the geometry of the magnet. Each counter will be 1 meter long and tapered so that it will be 14 cm wide at the outer radius and 2 cm wide at the inner radius of the detector.

Inside each one of the six air gaps, we will insert a set of scintillation counters. There will also be scintillation counters appropriately positioned upstream and downstream of the interaction region. Based on the experience at CERN-ISR, these counters are most crucial to insure that the event trigger originates from beam - beam interaction.

(4) The Lead Glass Hodoscope

The lead glass hodoscope will consist of 200 cells each of dimensions 10 cm x 10 cm laterally and 35 cm axially. Each cell will be viewed by a 2" diameter photomultiplier. The lead glass unit can be arranged to match the wheel shaped geometry of the air gaps of the magnetic detector.

Finally, we should remark that there exist a great number of spectrometer designs in various colliding - beam facility studies. They are all more or less similar. The distinctive feature of this proposed spectrometer lies in the fact that the magnet is toroidal with air gaps. These air gaps allow the detection of $e^{\pm}$ and charged hadrons. Also, at the price of sacrificing approximately one-third of the interaction region, the spectrometer provides good angular and momentum resolution. An alternative configuration, shown schematically in Figure 3, is also under consideration. In this arrangement, three magnets are used. The central magnet has two air gaps instead of six. The two end magnets are similar to that used in a CERN-ISR experiment. (See also a design study by Cheng, Goulianos, Knapp, Rosen and Schlein, 1975 Isabelle Summer Study at BNL, Vol. II, p.319).

III. The Trigger

The lepton trigger will consist of any of the possible pairs of particles (e^+e^-), $(\mu^+\mu^-)$, $(e^\pm\mu^\mp)$ or any combination of leptons greater than two. The lepton counters defining a wedge of the magnetic detector in each hodoscope bank will be in electronic "OR". A charged particle passing through the detector will then be defined by a coincidence of the counters in the two hodoscopes before and after the magnet defining an individual wedge. For charged particles passing through an iron wedge, this coincidence requirement is sufficient to identify them as muons. To form a single electron trigger, the charged particle trigger for an air gap will be placed in coincidence with a pulse in the lead glass of sufficient size to separate electrons from minimum ionizing particles. The experimental event trigger will then consist of a coincidence between any of the possible six muon triggers and any of the possible six electron triggers. The "beam - beam" interaction counters are also required in the final coincidence.

The possibility of triggers on single leptons will also be investigated empirically.

A certain amount of data will have to be taken triggering on single and double hadrons as well. This will be necessary to understand the background.

IV. Estimates of Counting Rates

The cross section for lepton pair production in pp collisions, in the parton-quark model,[1] is given by

$$\frac{d\sigma}{dm_{\ell\bar{\ell}}} = \frac{8}{3} \frac{\pi\alpha^2}{m_{\ell\bar{\ell}}^3} \int_0^1 dx_1 \int_0^1 dx_2 \;\; \delta(x_1 x_2 - \tau) \; x_1 x_2 \; f(x_1, x_2)$$

where $\tau \equiv \frac{m_{\ell\bar{\ell}}^2}{S}$

$$\begin{aligned} f(x_1,x_2) = & \left[\tfrac{4}{9} \;\; u(x_1)\,\bar{u}(x_2) + u(x_2)\,\bar{u}(x_1)\right] \\ & + \left[\tfrac{1}{9} \;\; d(x_1)\,\bar{d}(x_2) + d(x_2)\,\bar{d}(x_1)\right] \\ & + \left[\tfrac{1}{9} \;\; s(x_1)\,\bar{s}(x_2) + s(x_2)\,\bar{s}(x_1)\right] \end{aligned}$$

This model is independent of the lepton type in the final state, so that we can use it to predict the cross sections for the production of electron, muon, and heavy lepton pairs. The electron and muon pairs can be observed directly, whereas the presence of the heavy lepton pairs, if they exist, can be detected by their decays into electrons and/or muons.

The universal scaling function, $m_{\ell\bar{\ell}}^3 \frac{d\sigma}{dm_{\ell\bar{\ell}}}$, is shown in Figure 4. The predictions of this model are in reasonable agreement with various experimental results measured at Fermilab and BNL, so that it can be used as the basis to estimate the counting rates for heavy particle productions in this proposal. We are aware of the facts that for low mass states this universal function underestimates the cross section by a factor of $\sim$25,[2] and also that the universal function may still be seriously modified by energy dependence. Figures 5 and 6 show the expected cross section for the lepton-pair production as a function of the invariant mass, and also the main ring energy.

The counting rate for lepton-pairs is obtained from the product of the cross section, luminosity and detection efficiency integrated over the energy range of the main accelerator. Assuming that the invariant cross section of heavy particle production is proportional to $\exp(-4X_{\parallel} - 1.6P_{\perp})$, we can calculate the acceptance of our apparatus for detecting the lepton pairs from the heavy particle decays. Figure 7 shows a typical acceptance distribution as a function of $X_{\parallel}$ and $X_{\perp}$, for a 5 GeV particle with the main ring operating at 400 GeV. The average acceptance of our proposed apparatus is approximately 10%. Figure 8 shows a typical counting rate distribution anticipated for the lepton pairs from a 5 GeV particle. This estimate is obtained by assuming a main ring ramp of 8 sec duration, a 1 sec flat-top at 400 GeV, and 360 main ring pulses per hour. Figure 9 shows the integrated counting rate as a function of the invariant mass.

These estimates of heavy particle production can also be used to indicate the sensitivity for detecting heavy leptons and charmed particles. In this case, we have to multiply the rates as shown in Figure 9, by the decay branching ratios.

V. Estimate of Background

The background to this experiment can be estimated as follows: The pion production is calculated by the following formula -

$$\frac{1}{\sigma_{pp}^{Total}} E_{\pi} \frac{d^3\sigma}{d\vec{p}_{\pi}^{\,3}} = 0.1 \exp\left[-4X_{\parallel} - 6.7\, P_{\perp}/S^{1/8}\right].$$

Figure 10 displays the counting rate/sec for inclusive pion production. Figure 11 displays the counting rate/sec in the detector due to single muons arising from the decay of charged pions of either sign. The charged pion rate in the detector is approximately 30,000/sec, which will yield only 70 single muon triggers/sec of either sign from pion decays in flight. The Dalitz electron pairs from the neutral pions are of approximately the same rate. Electrons and muons from kaon decays are at the 10% level as that from the pions. It is shown that none of these rates will cause extreme difficulties to the experiment.

There is no easy way to estimate the background produced by halo, beam-gas and beam - pipe interactions. The counters, installed upstream and downstream of the interaction region with the requirement to detect oppositely going particles, will reduce the background from these sources to a negligible level. Since it is possible to locate the interaction point precisely using the rf structure of the main accelerator, we do not anticipate any serious problem with background.

VI. Request

We request one year of running time on the SSR to search for new heavy particles.

REFERENCES

1. S. Pakvasa, D. Parashar, and S.F. Tuan, Phys. Rev. D10, 2124(1974).
R.B. Palmer, E.A. Paschos, N.P. Samios, and L.L. Wang, Preprint BNL-20634 (1976).

2. J.D. Bjorken and H. Weisberg, SLAC Report SLAC-PUB-1631 (1975).

FIGURE CAPTIONS

Fig. 1a Schematic of the spectrometer.

Fig. 1b End view of magnet.

Fig. 2a Schematic arrangement of a drift chamber module.

Fig. 2b Schematic of wire layout of drift chamber.

Fig. 3 Schematic configuration of a three - magnet spectrometer. The beam goes through a hole in the center of the middle septum of each end magnet.

Fig. 4 The universal scaling function $m^3_{\ell\bar{\ell}} \frac{d\sigma}{dm_{\ell\bar{\ell}}}$.

Fig. 5 Cross-sections for lepton-pair production as a function of the invariant mass.

Fig. 6 Cross-sections for lepton pair production as a function of the main ring energy.

Fig. 7 Detection efficiency in per cent for di-lepton pairs as a function of $X_{\parallel}$ and $X_{\perp}$ of the parent particle. The numbers are for the typical case of 25 GeV x 400 GeV and for a di-lepton mass of 5 GeV.

Fig. 8 Counting Rate/GeV/Hour as a function of $X_{\parallel}$ and $X_{\perp}$ of a 5 GeV di-lepton produced in 25 GeV x 400 GeV collisions. (Calculation for a 1 sec flattop and 360 pulses/hour). If both muon and electron pairs are detected, these numbers should be multiplied by two.

Fig. 9 Total counting rate/GeV/hour as a function of di-lepton mass. If both muon and electron pans are detected, these numbers should be multiplied by two.

Fig. 10 Counting rate/sec for inclusive π production of one charge produced in 25 GeV x 400 GeV collisions as a function of $X_{\parallel}$ and $X_{\perp}$ of the pion.

Fig. 11 Counting rate/sec of single muons arising from the decay of pions in flight as a function of $X_{\parallel}$ and $X_{\perp}$ of the pion. The pions are produced in an interaction of 25 GeV protons with 400 GeV protons.

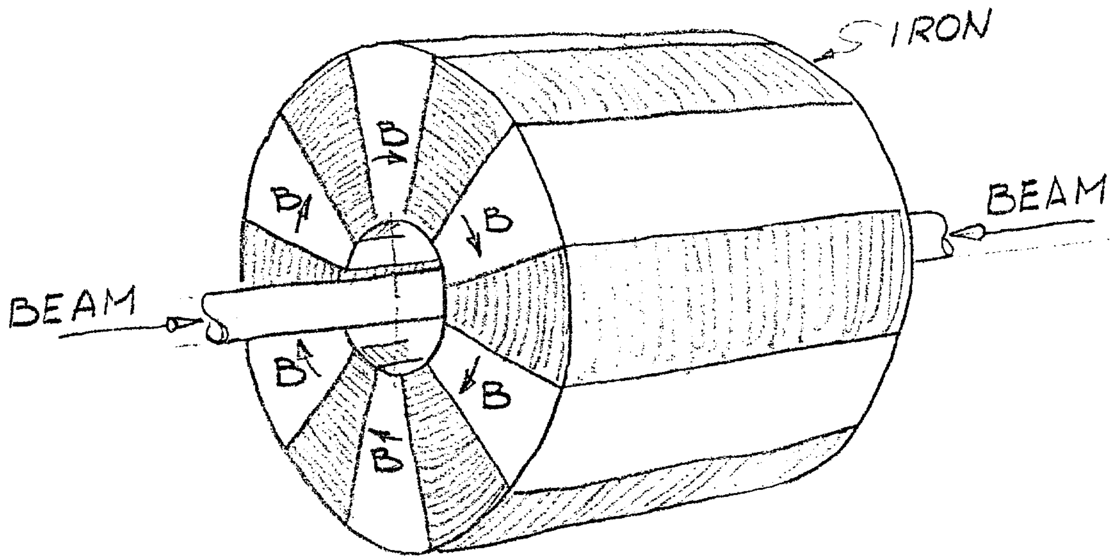

Wheel Magnet (Coils and support not shown)

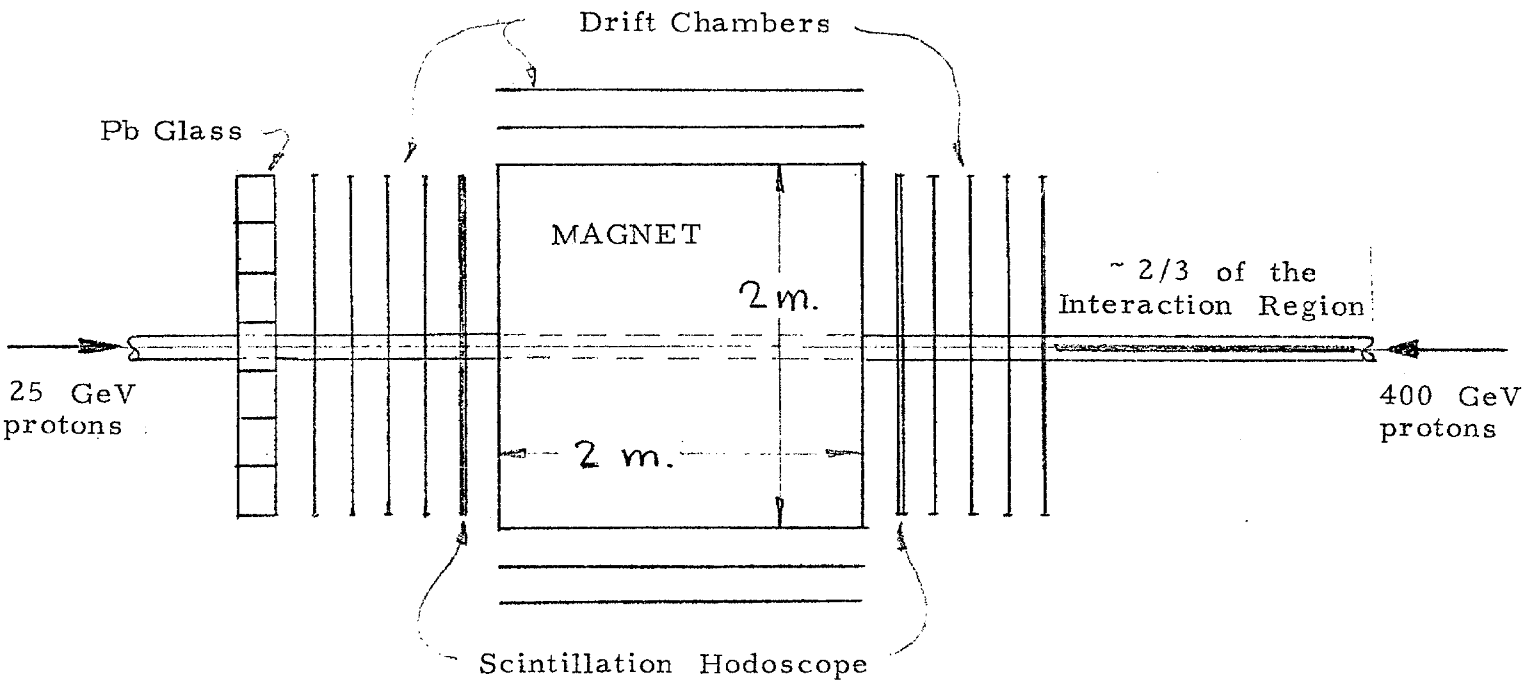

SCHEMATIC

Fig. 1a

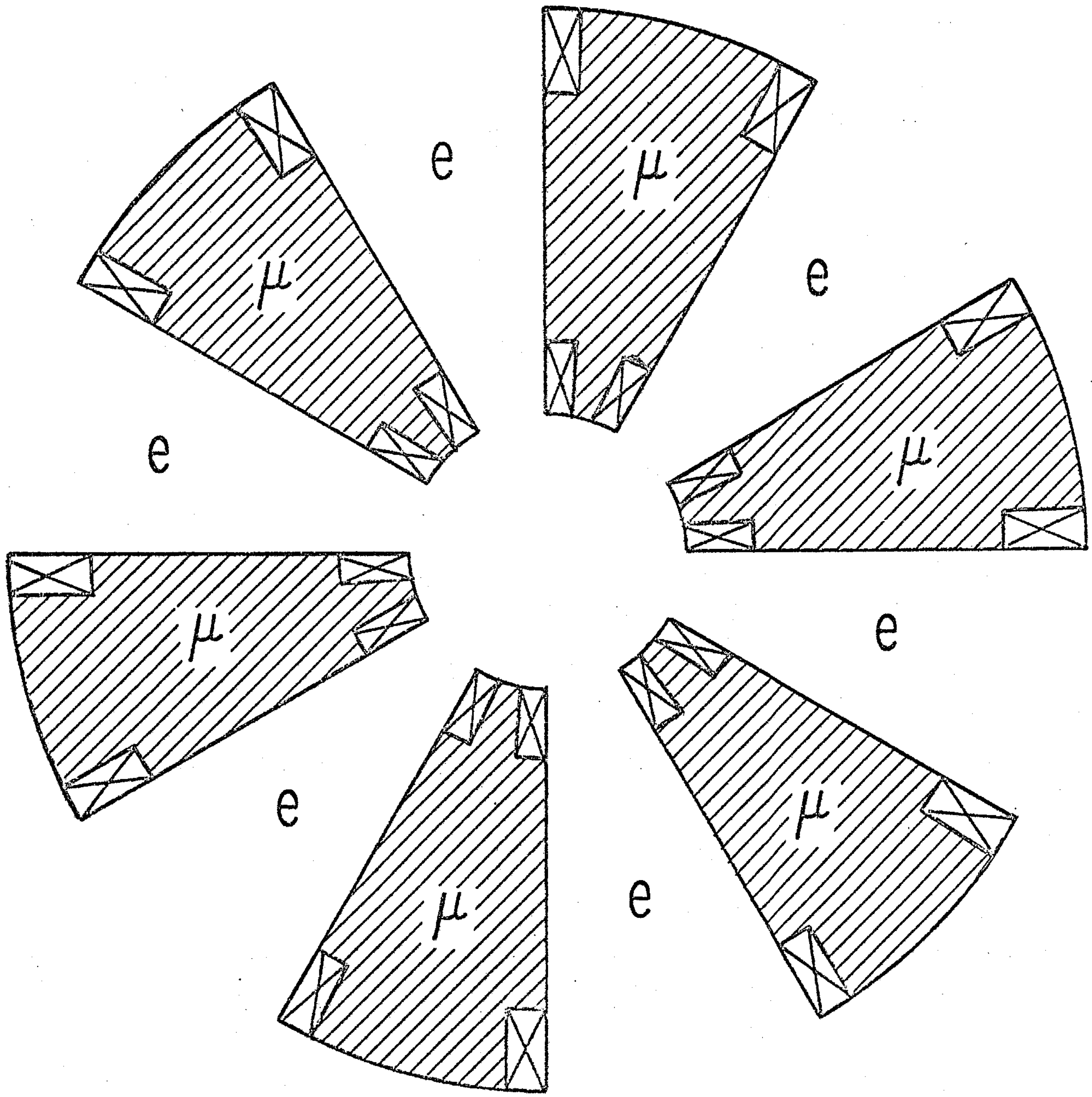

Fig. 1b

480-13

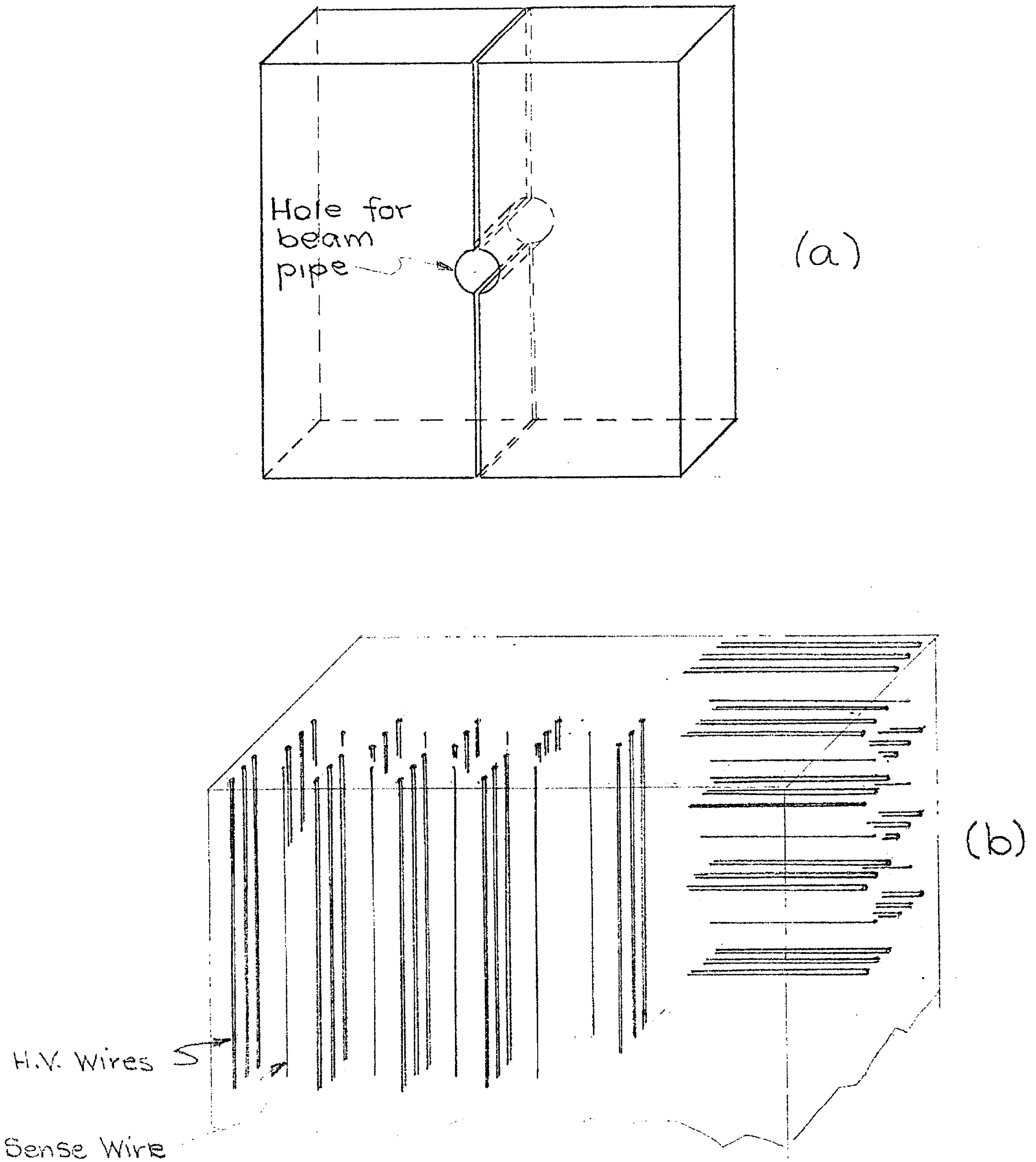

Fig. 2

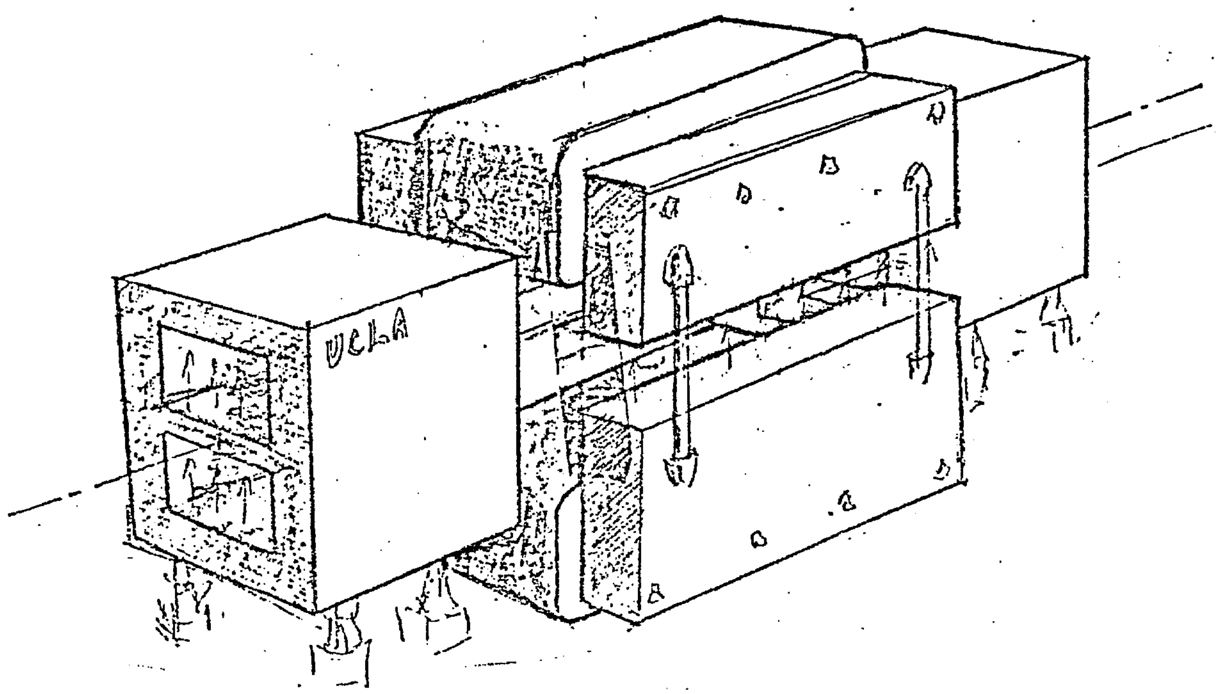

Fig. 3

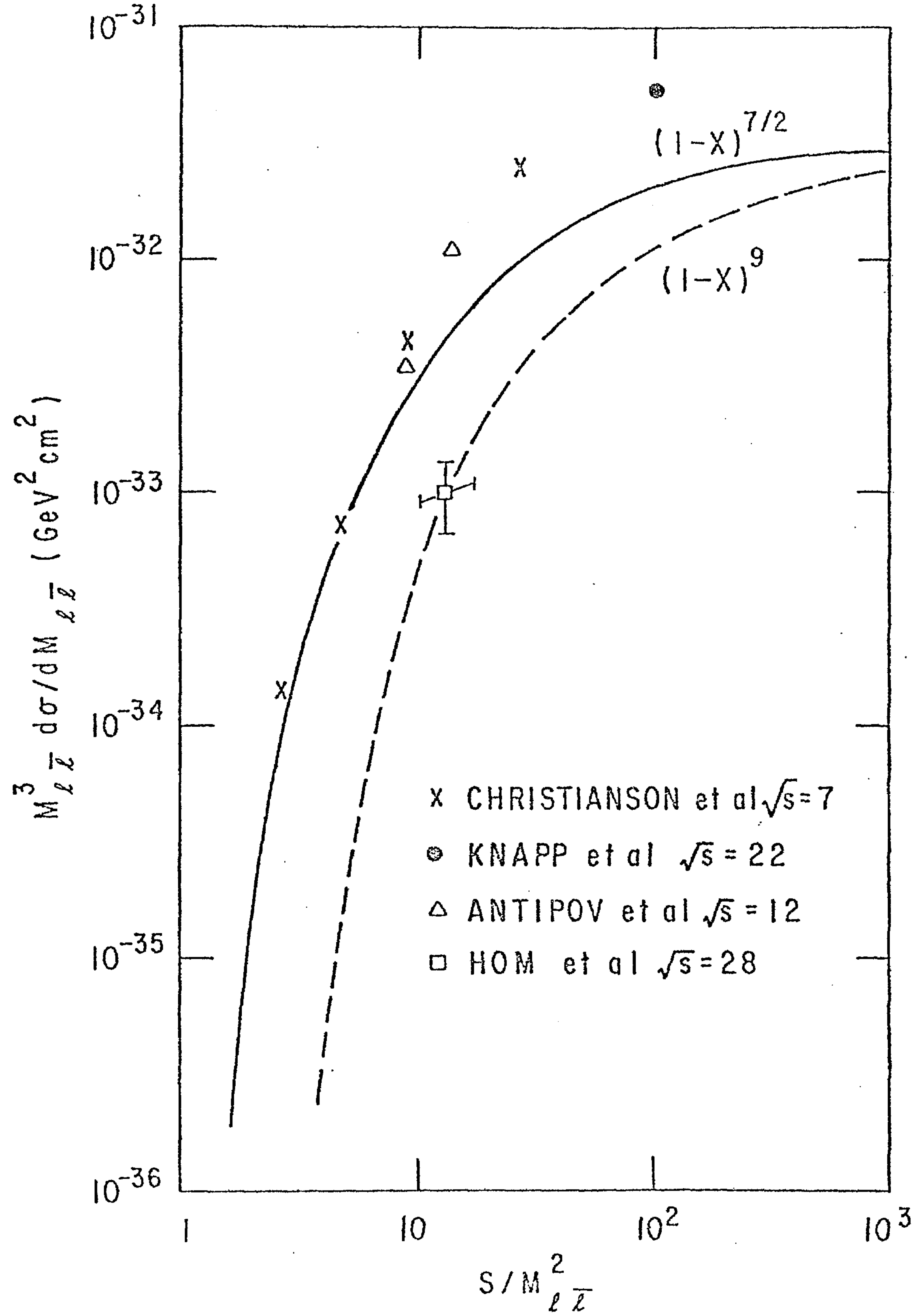

10^{-31}
10^{-32}
10^{-33}
10^{-34}
10^{-35}
10^{-36}
$M^3_{\ell\bar{\ell}}\ d\sigma/dM_{\ell\bar{\ell}}$ (GeV^2 cm^2)
$(1-X)^{7/2}$
$(1-X)^9$
X CHRISTIANSON et al $\sqrt{s}=7$
KNAPP et al $\sqrt{s}=22$
△ ANTIPOV et al $\sqrt{s}=12$
□ HOM et al $\sqrt{s}=28$
1
10
10^2
10^3
$S/M^2_{\ell\bar{\ell}}$

Fig. 4

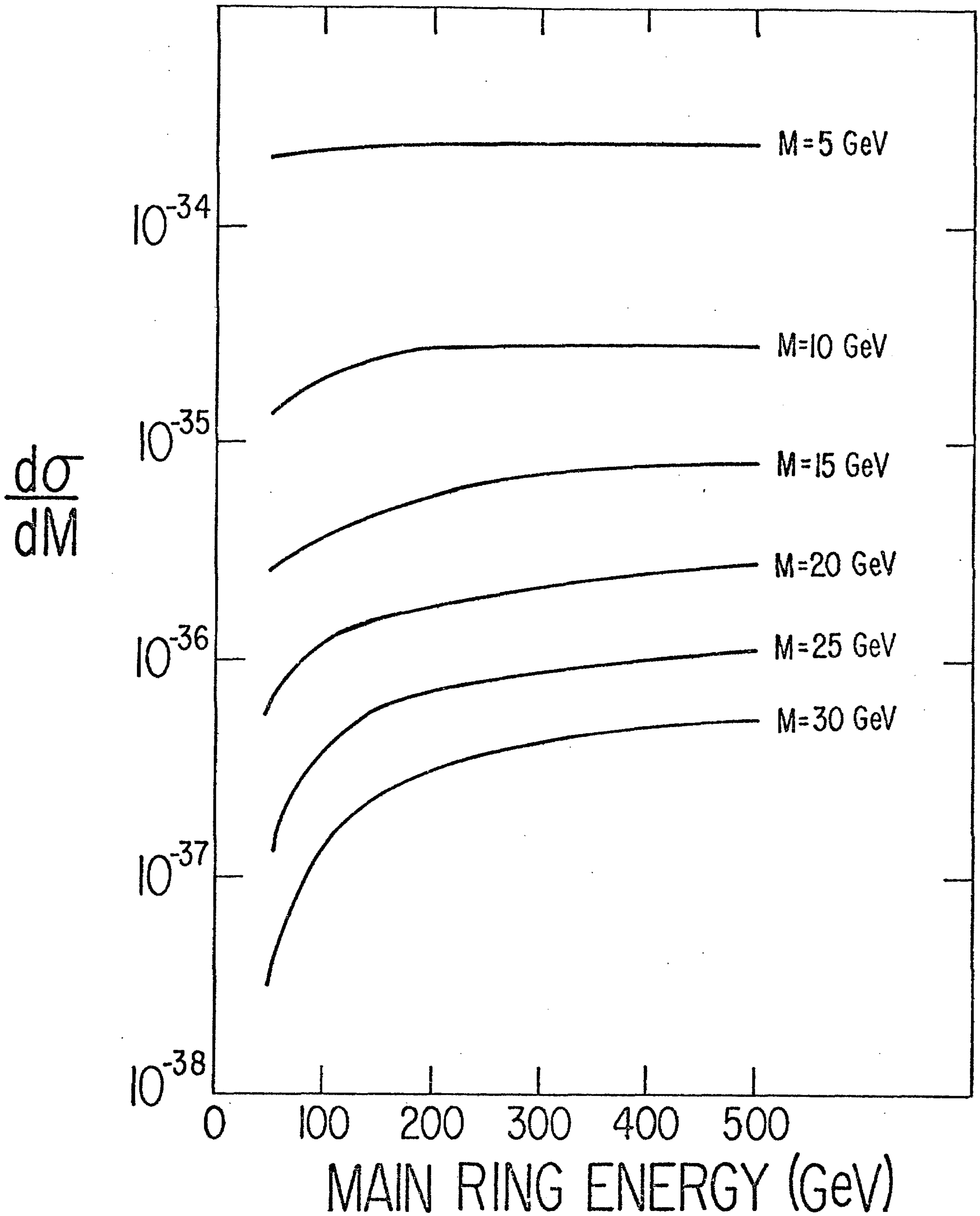
M=5 GeV
M=10 GeV
M=15 GeV
M=20 GeV
M=25 GeV
M=30 GeV
10^{-34}
10^{-35}
10^{-36}
10^{-37}
10^{-38}
$\frac{d\sigma}{dM}$
0
100
200
300
400
500
MAIN RING ENERGY (GeV)

Fig. 5

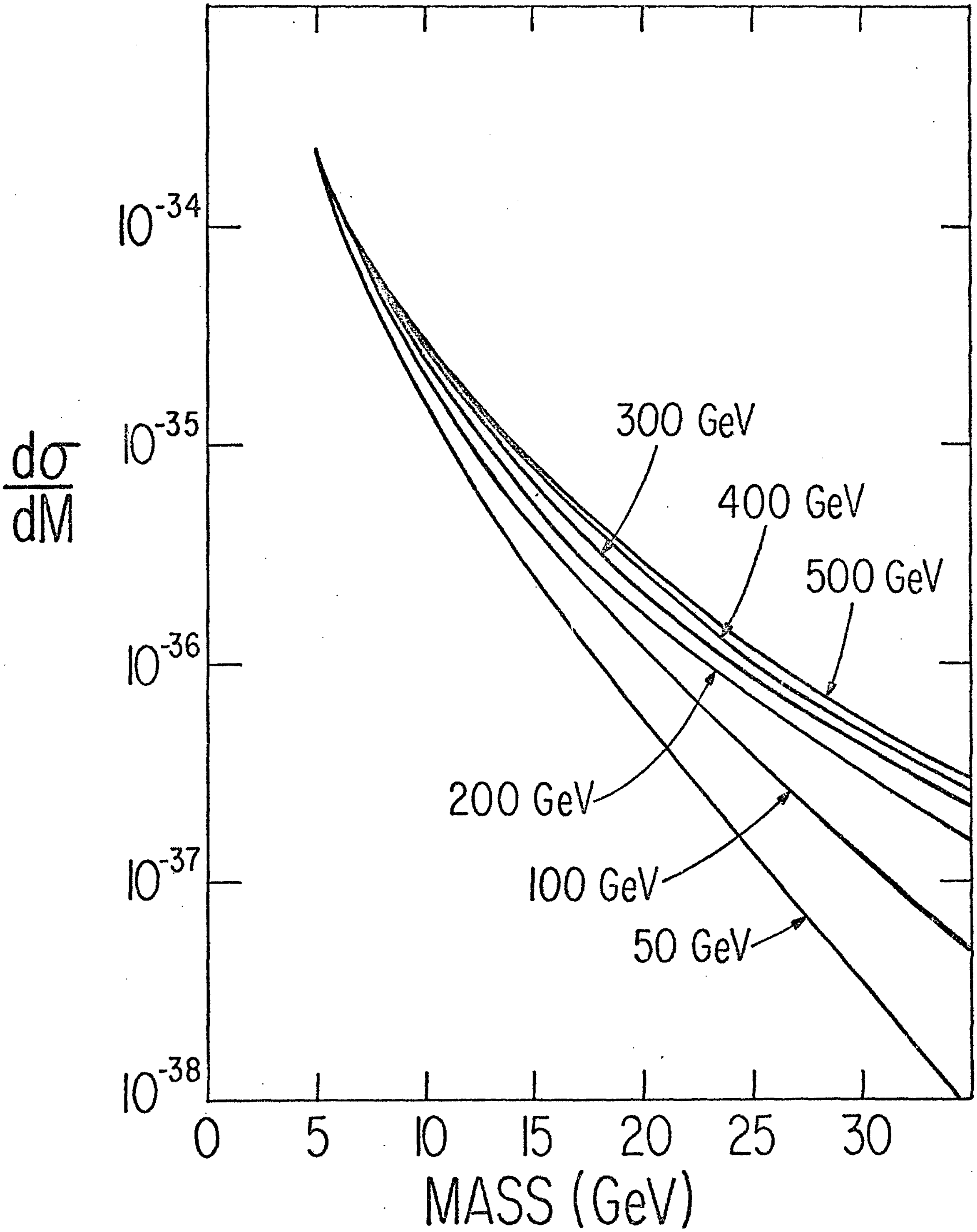
$\frac{d\sigma}{dM}$
10^{-34}
10^{-35}
10^{-36}
10^{-37}
10^{-38}
300 GeV
400 GeV
500 GeV
200 GeV
100 GeV
50 GeV
0
5
10
15
20
25
30
MASS (GeV)

Fig. 6

480-19

$x_{\parallel}$ of di-lepton \ $x_{\perp}$ of di-lepton	0–0.01	0.01–0.02	0.02–0.03	0.03–0.04	0.04–0.05	0.05–0.06	0.06–0.07	0.07–0.08	0.08–0.09	0.09–0.1
−0.1–0.0						0.1	0.1	0.2	0.2	0.2
0.0–0.1	2.2	2.2	2.1	2.0	1.8	1.7	2.0	2.5	2.8	3.1
0.1–0.2	12	11	10	8.8	7.5	7.6	8.3	8.9	9	9
0.2–0.3	22	21	19	17	14	15	17	16	16	16
0.3–0.4	25	24	22	18	16	19	22	23	23	24
0.4–0.5	26	22	20	17	16	20	25	26	26	28
0.5–0.6	19	20	19	17	16	19	23	26	28	31
0.6–0.7	15	15	15	15	14	17	21	25	27	30
0.7–0.8	11	11	13	13	13	14	19	22	27	29
0.8–0.9	7.1	7.1	9.2	12	12	12	17	21	25	28
0.9–1.0	3.1	3.1	6.1	9.2	11	11	13	19	22	27

Fig. 7

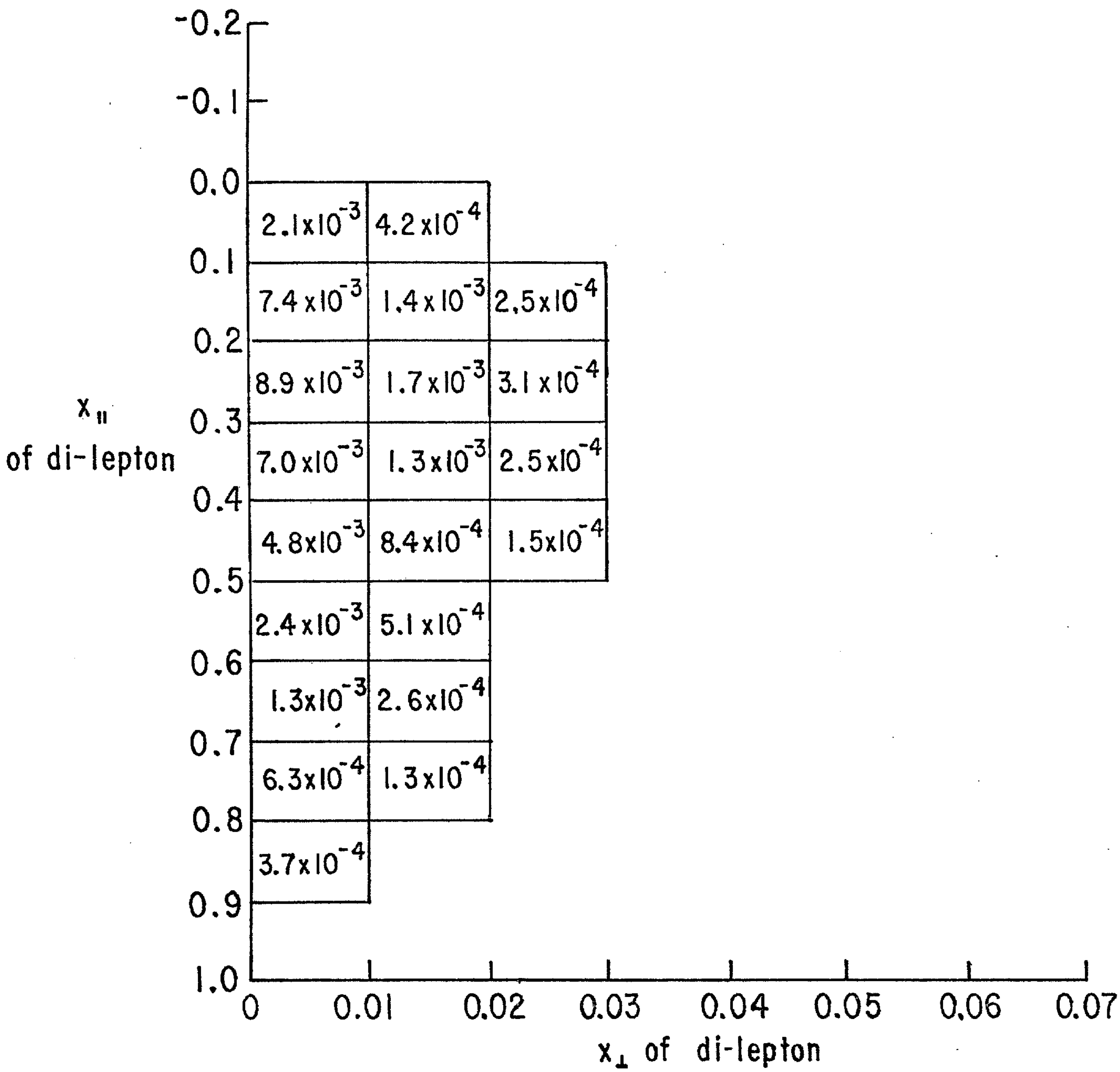
-0.2
-0.1
0.0
0.1
0.2
0.3
0.4
0.5
0.6
0.7
0.8
0.9
1.0
$x_{\parallel}$ of di-lepton
2.1x10^-3
4.2x10^-4
7.4x10^-3
1.4x10^-3
2.5x10^-4
8.9x10^-3
1.7x10^-3
3.1x10^-4
7.0x10^-3
1.3x10^-3
2.5x10^-4
4.8x10^-3
8.4x10^-4
1.5x10^-4
2.4x10^-3
5.1x10^-4
1.3x10^-3
2.6x10^-4
6.3x10^-4
1.3x10^-4
3.7x10^-4
0
0.01
0.02
0.03
0.04
0.05
0.06
0.07
$x_{\perp}$ of di-lepton

Fig. 8

480-21

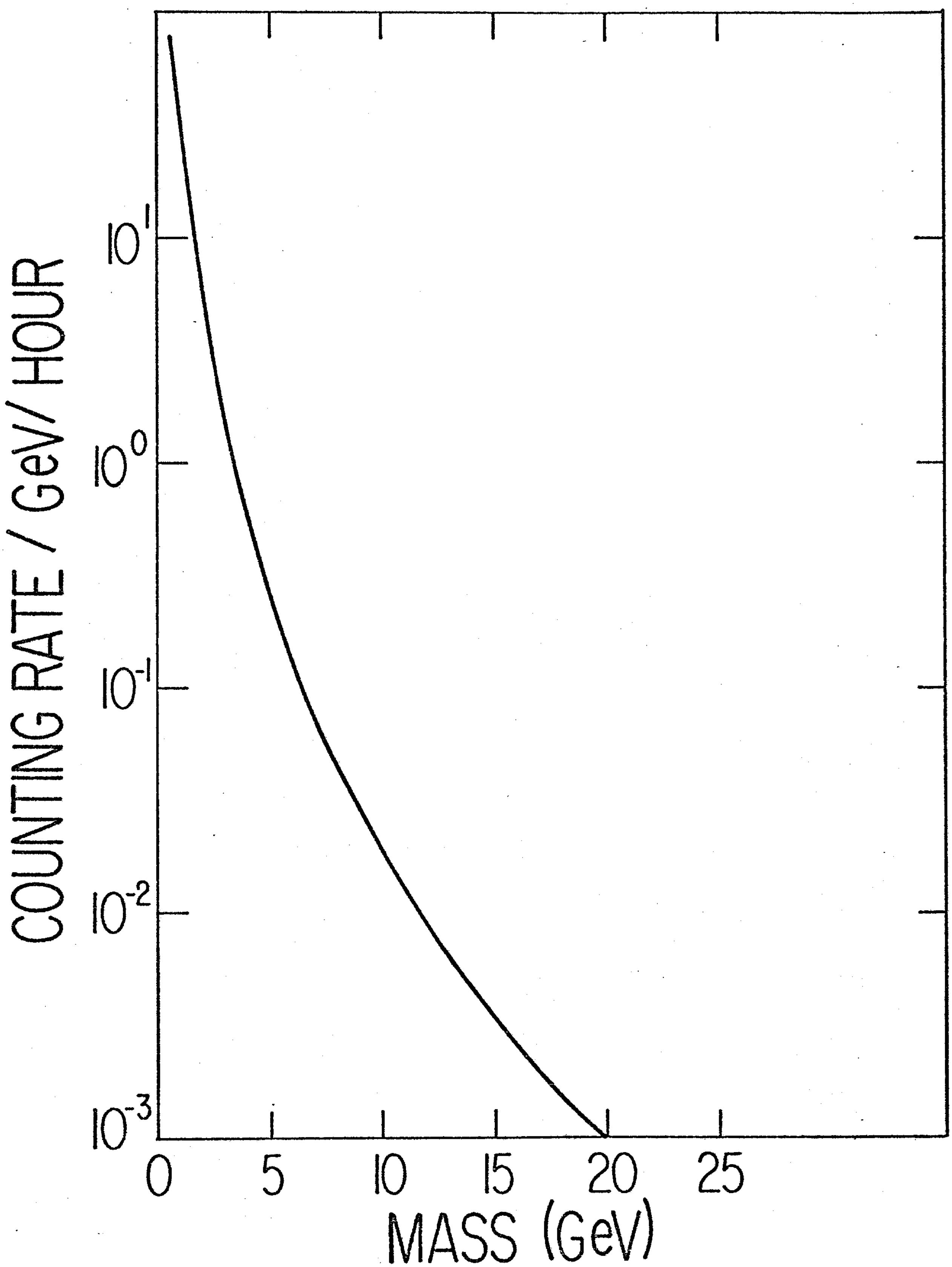

COUNTING RATE / GeV/ HOUR
10^1
10^0
10^{-1}
10^{-2}
10^{-3}
0
5
10
15
20
25
MASS (GeV)

Fig. 9

480-22

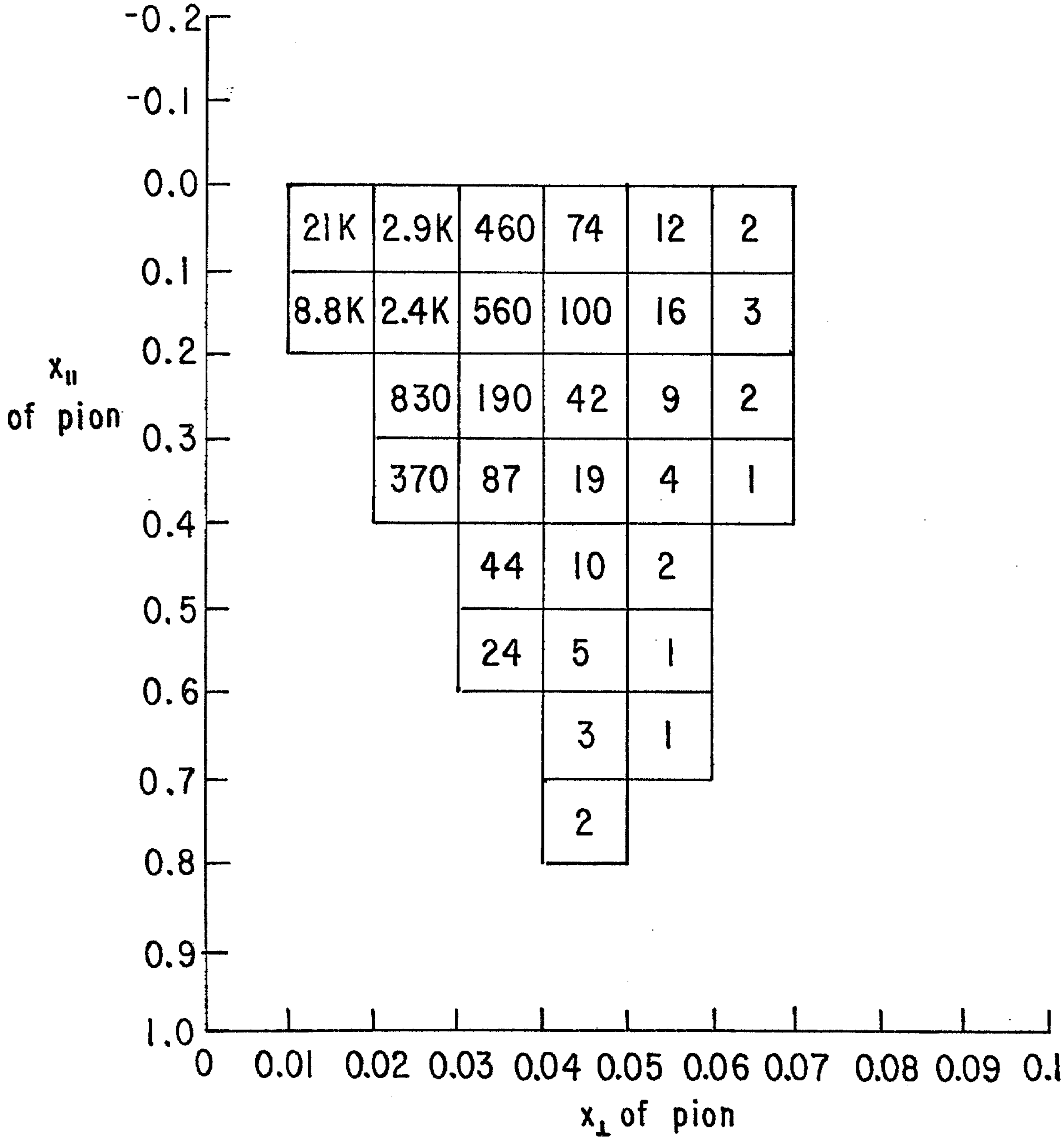

-0.2
-0.1
0.0
0.1
0.2
0.3
0.4
0.5
0.6
0.7
0.8
0.9
1.0
$x_{\parallel}$ of pion
21K
2.9K
460
74
12
2
8.8K
2.4K
560
100
16
3
830
190
42
9
2
370
87
19
4
1
44
10
2
24
5
1
3
1
2
0
0.01
0.02
0.03
0.04
0.05
0.06
0.07
0.08
0.09
0.1
$x_{\perp}$ of pion

Fig. 10

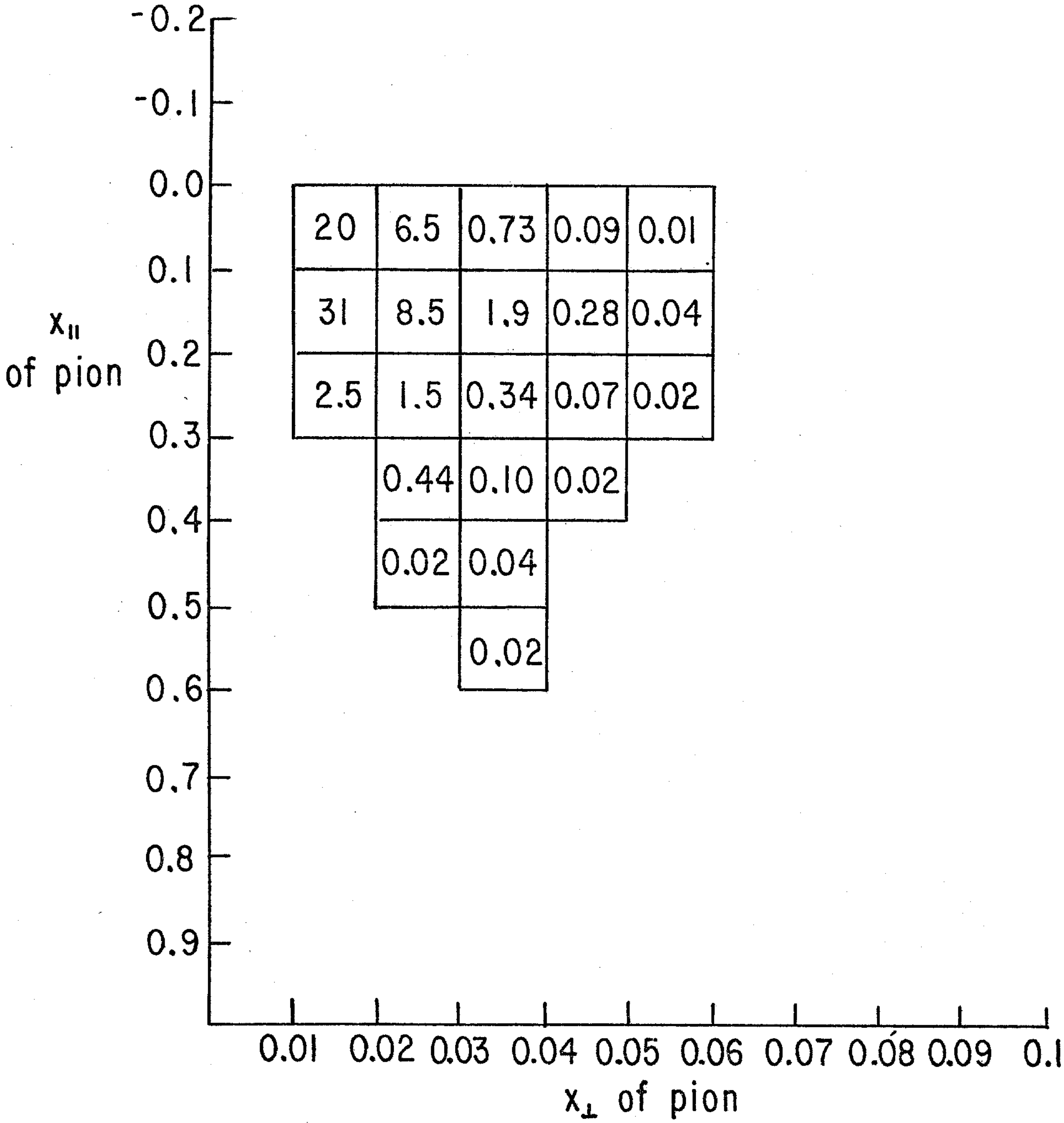
-0.2
-0.1
0.0
0.1
0.2
0.3
0.4
0.5
0.6
0.7
0.8
0.9
x‖
of pion
20
6.5
0.73
0.09
0.01
31
8.5
1.9
0.28
0.04
2.5
1.5
0.34
0.07
0.02
0.44
0.10
0.02
0.02
0.04
0.02
0.01
0.02
0.03
0.04
0.05
0.06
0.07
0.08
0.09
0.1
x⊥ of pion

Fig. 11